Errata:
"Nonlinear surface acoustic waves in cubic crystals"

Ronald E. Kumon

October 16, 2001

This document lists errata for my dissertation [1]. Most errors are typographical in nature; those which are more significant are marked by asterisks. Other errors may still exist, and this list may be updated as these errata are identified. If you think you have identified an error in the dissertation which is not on this list (or an error in this errata), please contact the author via electronic mail at *kumon@apsmail.org*.

p. 12: In the first line of the first full paragraph, "has" should be replaced by "have."

p. 29: In Eq. (2.15), c_{ijklmn} should be replaced by d_{ijklmn}.

p. 72: In the eighth line of the paragraph, "elastic" should be deleted.

p. 77: In the table, the entry for the row "Ni" and column "d_{144}" of "-180" should be replaced by "-180."

p. 78: In the headings of both tables "$\bar{3}m$" should be replaced by "$m\bar{3}$."

p. 96: In the third line of the first full paragraph, "Eqs. 2.40" should be replaced by "Eqs. (2.40)." In the last sentence on the page, the phrase "of Eq. (2.41)" should be deleted, and Eq. (4.7) should be replaced by

$$V_j(X, 0, \tau) = \sum_{n=1}^{\infty} V_n(X) B_j e^{-in\omega\tau} \,,$$

where $\tau = t - x/c$.

p. 99: In the second line of the first list item, "$B_3 = 0$" should be replaced by "$B_2 = 0$."

p. 101: On the second line of the list item, "$S_{11}(35°)/S_1(0°)$" should be replaced by "$|\widehat{S}_{11}(35°)|/|\widehat{S}_{11}(0°)|$." Also, in the second sentence of the first full paragraph, "$u_0 = v_0/\omega_0$" should be replaced by "$u_0 = 2v_0/\omega_0$." (The original intention was to scale by $u_0 = v_0/\omega_0$, but an extra factor of $1/2$ was erroneously included in the computation of the displacement waveforms.)

p. 102: The displacement waveforms should really have the DC component filtered out ($U_j = U_j^{\text{fig}} - \overline{U_j^{\text{fig}}}$) where U_j^{fig} are the displacement components shown in the figure). See also the second sentence of the errata for p. 101 for the proper scaling factor for all the displacement components.

p. 103: See the second sentence of the errata for p. 101 for the proper scaling factor for all the particle trajectories.

***p. 106:** In the key of Fig. 4.9, "Drabble and Strathen" should be replaced by "Drabble and Gluyas."

***p. 109:** In the sixteenth line of the first list item, "Figure 4.12" should be replaced by "Figure 4.11."

***p. 112:** In the third line of the second list item, "$|\widehat{S}_{13}|/|\widehat{S}_{11}|$" should be replaced by "$|\widehat{S}_{12}|/|\widehat{S}_{11}|$."

p. 126: In the second line from the bottom of the page, "0° to 45° from $\langle 100 \rangle$" should be replaced by "0° to 90° from $\langle 001 \rangle$.'

p. 128: In the fourth line of the second paragraph, "occurs" should be replaced by "occur."

****p. 129:** The graphs are incomplete. Figure 14 shows the revised graphs for Cs-alum, K-alum, and NH_4-alum. The phases of the nonlinearity matrix elements are periodic every 360°. However, the magnitudes of nonlinearity matrix elements are still periodic every 180° and symmetric about the bisector of each 180° period. See the appendix for additional discussion of the periodicity of the linear and nonlinear SAW parameters for crystals in the $m\bar{3}$ point group.

p. 133: The displacement waveforms should really have the DC component filtered out ($U_j = U_j^{\text{fig}} - \overline{U_j^{\text{fig}}}$) where U_j^{fig} are the displacement components shown in the figure). See also the second sentence of the errata for p. 101 for the proper scaling factor for all the displacement components.

p. 134: See the second sentence of the errata for p. 101 for the proper scaling factor for all the particle trajectories.

p. 149: The following sentence should be added to the figure caption: "The SAW speed of each material is measured relative to $c_{\text{ref}} = (c_{44}/\rho)^{1/2}$, and the speed is periodic every 60°."

****p. 152:** The graphs are incomplete. Figure 1 shows the revised graphs for RbCl, KCl, NaCl, CaF_2, SrF_2, and BaF_2. While the magnitudes of the nonlinearity matrix elements are periodic every 60°, the phases of the nonlinearity matrix elements are periodic every 120°. Note that the graphs only show the values of the nonlinearity matrix elements from 0° to 60° because the graphs are symmetric about the 60° direction. See the appendix for additional discussion of the periodicity of the linear and nonlinear SAW parameters of

crystals in the $m\bar{3}m$ point group. [Thanks to A. Lomonosov for identifying this error.]

****p. 153:** The graphs are incomplete. Figure 2 shows the revised graphs for C, Si, Ge, Al, Ni, and Cu. While the magnitudes of the nonlinearity matrix elements are periodic every 60°, the phases of the nonlinearity matrix elements are periodic every 120°. Note that the graphs only show the values of the nonlinearity matrix elements for 0° to 60° because the graphs are symmetric about the 60° direction. See the appendix for additional discussion of the periodicity of the linear and nonlinear SAW parameters of crystals in the $m\bar{3}m$ point group. [Thanks to A. Lomonosov for identifying this error.]

****p. 154:** The graphs are incomplete. Figure 11 shows the revised graphs for Cs-alum, K-alum, and NH_4-alum. While the magnitudes of the nonlinearity matrix elements are periodic ever 60°, the phases of the nonlinearity matrix elements are periodic every 120°. [Thanks to A. Lomonosov for identifying this error.] In contrast to the materials shown on p. 152–153, the nonlinearity matrix elements are not symmetric about the 60° direction. This difference occurs because the alums are in the $m\bar{3}$ point group while the other materials are in the higher symmetry $m\bar{3}m$ point group. See the appendix for additional discussion of the periodicity of the linear and nonlinear SAW parameters of crystals in the $m\bar{3}$ point group.

p. 154: In the eighth line of text, "SAWs in crystal" should be replaced by "SAWs in a crystal."

p. 159: In the fifth line of the first paragraph, "elastic" should be deleted.

p. 160: In the caption of the figure, "$0 \leq \theta \leq 180°$" should be replaced by "$0° \leq \theta \leq 180°$," "$\theta = 0$" should be replaced by "$\theta = 0°$," and "$\theta = 180$" should be replaced by "$\theta = 180°$."

p. 161: In the caption of the figure, "$-180° \geq \theta \geq 0$" should be replaced by "$-180° \leq \theta \leq 0°$" "$\theta = 0$" should be replaced by "$\theta = 0°$," and "$\theta = -180$" should be replaced by "$\theta = -180°$."

p. 162: In the sixth line of the first full paragraph, "phase" should be replaced by "phases."

****p. 166:** The last sentence of the first list item is incorrect. It should replaced with the sentences: "The magnitudes of the matrix elements are periodic every 60° and symmetric about the bisector of each 60° period. However, the phases of the matrix elements are periodic every 120° and symmetric about the bisector of each 120° period." See the appendix for additional discussion of the periodicity of the linear and nonlinear SAW parameters. [Thanks to A. Lomonosov for identifying this error.]

****p. 167:** The graphs are incomplete. Figure 8 shows an updated version of the graphs for Si (replacing the graphs of $|\beta|$ and x_{shock} with those for $|l_3^{(s)}|$ and $\arg[l_3^{(s)}]$). The phases of the nonlinearity matrix elements S_{lm} are periodic every 120° and symmetric about the bisector of each 120° period. However, their magnitudes are still periodic every 60° and symmetric about the bisector of each 60° period. In addition, the complex-valued lower half-plane roots of the secular equation have the same symmetries as the nonlinearity matrix. The

component amplitudes B_j/B_0 are periodic every 60° in magnitude and every 120° in phase. In addition, the last sentence of the caption in Fig. 6.9 should be replaced by the sentences: "The phases $\arg(-S_{lm}/c_{44})$ are periodic every 120° and symmetric about the bisector of each 120° period. The phases $\arg(B_j/B_0)$ are periodic every 120°. All other parameters shown are periodic every 60° and symmetric about the bisector of each 60° period." See the appendix for additional discussion of the periodicity of the linear and nonlinear SAW parameters of crystals in the $m\bar{3}m$ point group. [Thanks to A. Lomonosov for identifying this error.]

p. 170: The displacement waveforms should really have the DC component filtered out ($U_j = U_j^{\text{fig}} - \overline{U_j^{\text{fig}}}$) where U_j^{fig} are the displacement components shown in the figure). See also the second sentence of the errata for p. 101 for the proper scaling factor for all the displacement components.

p. 171: See the second sentence of the errata for p. 101 for the proper scaling factor for all the particle trajectories.

p. 176: In the fourth line of Section 6.2.4, the word "they" should be deleted.

****p. 177:** The graphs are incomplete. (See the comments above about the errata on p. 167.) Figure 9 shows an updated version of the graphs for KCl (replacing the graphs of $|\beta|$ and x_{shock} with those for $|l_3^{(s)}|$ and $\arg[l_3^{(s)}]$). The last sentence of the caption in Fig. 6.14 should be replaced by the sentences: "The phases $\arg(-S_{lm}/c_{44})$ are periodic every 120° and symmetric about the bisector of each 120° period. The phases $\arg(B_j/B_0)$ are periodic every 120°. All other parameters shown are periodic every 60° and symmetric about the bisector of each 60° period." See the appendix for additional discussion of the periodicity of the linear and nonlinear SAW parameters of crystals in the $m\bar{3}m$ point group. [Thanks to A. Lomonosov for identifying this error.]

****p. 184:** The graphs are incomplete. (See the comments above about the errata on p. 167.) Figure 10 shows an updated version of the graphs for Ni (replacing the graphs of $|\beta|$ and x_{shock} with those for $|l_3^{(s)}|$ and $\arg[l_3^{(s)}]$). The last sentence of the caption in Fig. 6.17 should be replaced by the sentences: "The phases $\arg(-S_{lm}/c_{44})$ are periodic every 120° and symmetric about the bisector of each 120° period. The phases $\arg(B_j/B_0)$ are periodic every 120°. All other parameters shown are periodic every 60° and symmetric about the bisector of each 60° period." See the appendix for additional discussion of the periodicity of the linear and nonlinear SAW parameters of crystals in the $m\bar{3}m$ point group. [Thanks to A. Lomonosov for identifying this error.]

***p. 266:** In the fourth line of the first paragraph of Section C.4, "more" should be replaced by"less."

p. 273: The direction of rotation of the angles θ should be reversed in the diagrams of the (110) and (111) planes. Figure 17 shows the corrected diagrams.

p. 279: In the third line of the second paragraph, "phase" should be replaced by "phases."

p. 320: In Ref. 330, ",1" after "7(1)" should be omitted.

A Periodicity of Linear and Nonlinear SAW Parameters in the (111) Plane of Cubic Crystals

This appendix discusses the periodicity of the various linear and nonlinear surface wave parameters in the (111) plane of cubic crystals. It investigates in more detail errata with double asterisks given in the main text.

A.1 Crystals in $m\bar{3}m$ Point Group

In the (111) plane, the nonlinearity matrix elements are also generally complex-valued for materials in the $m\bar{3}$ point group. Figures 1 and 2 show the nonlinearity matrices plotted for selected crystals. In all these materials the magnitude of the nonlinearity matrix elements are periodic every 60° and symmetric about the bisector of each 60° period. In contrast, the phase of the nonlinearity matrix elements are periodic every 120° and symmetric about the bisector of each 120° period. As such, it is only neccesary for the graphs to plot from 0° to 60°.

One consequence of this result is that the waveform distortion would be expected to be different in the direction $[11\bar{2}]$ (0°) and the opposite direction $[\bar{1}\bar{1}2]$ ($180° \equiv 60°(\mathrm{mod}\,120°)$]. This behavior has been observed by A. Lomonosov in crystalline silicon [2].

The nonlinearity matrix elements are functions of both parameters from the nonlinear problem (e.g., the third-order elastic constants) and parameters from the linearized problem (e.g., second-order elastic constants, the eigenvalues and eigenvectors of the secular equation). As shown below, the threefold periodicity of the phase of the nonlinearity matrix elements is not strictly a nonlinear effect but occurs because several the linear parameters also have threefold periodicity in phase.

It appears that Farnell [3] did not notice this result in his review article on surface waves in crystals. In Sec. V.D. of the cited article, he discusses numerical results in the (111) plane of cubic crystals. At the end of the first paragraph of this section, he writes:

> The root locations as a function of angle for propagation on this plane with nickel and KCl, respectively, as the medium are plotted in Figs. 15 and 16, while Fig. 17 shows the corresponding velocities. Such curves all have mirror symmetry about the 30° direction and sixfold symmetry in general on this surface. (pp. 132–133 of Ref. [3])

Figs. 15 and 16 from the Farnell article are reproduced in Figs. 3 and 4 here. The density and elastic constant data used to generate the plots are deduced from Table I of Farnell's article, and differ slightly from those used in the dissertation [1]. For reference, Farnell uses $\rho = 8914.3$ kg/m^3, $c_{11} = 261$ GPa, $c_{12} = 151$ GPa, and $c_{44} = 130.9$ GPa for Ni and

$\rho = 1988.4$ kg/m^3, $c_{11} = 398$ GPa, $c_{12} = 62$ GPa, and $c_{44} = 63$ GPa for KCl. Note that Farnell denotes the angle of propagation from [110] instead of [112], as done in Figs. 1–2. Also recall that linear SAWs can be written in the form

$$u_j = \sum_{n=1}^{3} \beta_j^{(n)} \exp[ik(l_1 x_1 + l_2 x_x + l_3^{(n)} x_3 - vt)] \,, \tag{1}$$

where $l_3^{(n)}$ are the lower half plane roots of the secular equation and $\beta_j^{(n)} = C_n \alpha_j^{(n)}$ are the factors which allow the surface wave to satisfy the stress-free boundary conditions.

Figs. 5 and 6 show the same graphs for Ni and KCl, respectively but with the upper limit of the angular range of directions extended from 30° to 120°. The figures show that while the imaginary parts of the roots (which characterize the depth decay envelope) are periodic every 60°, the real parts (which characterize the oscillations with depth) are periodic every 120°. While there is some arbitrariness in ordering the roots, there is no way to order them such that all the real and imaginary parts are periodic every 60°. The roots do show mirror symmetry about the bisectors of each individual 60° interval shown, but not about the bisector of the full 120° period. Although the lower half-plane roots of Si exhibit the same trends as Ni, they are shown in Fig. 7 for completeness.

The same lower half-plane roots are plotted in a somewhat different form in Figs. 8–10. Graphs (g) and (h) in these figures show the magnitudes $|l_3^{(n)}|$ and phases $\arg[l_3^{(n)}]$. The advantage of plotting the parameters in this way is that it shows the magnitudes are periodic every 60° while the phases are periodic every 120° just like the nonlinearity matrix elements.

At the surface, the factors which describe relative magnitude and phase of the components of the SAW are

$$B_j = |B_j| e^{i\phi_j} = \sum_{n=1}^{3} \beta_j^{(n)} \,. \tag{2}$$

Graphs (c) and (d) in Figs. 8–10. show the magnitudes $|B_j/B_0|$ and phases ϕ_j, where $|B_0|^2 = |B_1|^2 + |B_2|^2 + |B_3|^2$ is the total magnitude. The B_j also exhibit 60° periodicity in the magnitudes and 120° periodicity in the phases. Note that, by convention, the absolute phases of the B_j are set such that $\phi_1 = -90°$. For reference, graphs (c) and (d) in Figures 1–3 are expanded versions of graphs (g) and (h) in Figs. 6.9, 6.17, and 6.14, respectively, of the dissertation.

The 120° periodicity of the phases of $l_3^{(n)}$ and B_j is important because the nonlinearity matrix is a function of these quantities [4]. Thus, given that the phases of these linear parameters have threefold symmetry, it is not unexpected that the phases of the nonlinearity matrix elements have the same symmetry.

Two linear SAW parameters do have sixfold symmetry. Graph (g) in Figs. 8–10 shows the SAW (solid) and the two quasitransverse bulk (long and short dashed) wave speeds are periodic every 60°. (Although not shown, the quasilongitudinal bulk wave is also periodic

over the same interval.) In addition, graph (h) in Figs. 8–10 shows that the angular deviation of the group velocity direction from the phase velocity direction also repeats every 60°. It may be that, because these two linear parameters are more easily measured experimentally than $l_3^{(n)}$ and B_j, it was assumed that all the linear parameters have the same periodicity. However, the above numerical investigation shows that this is not the case.

A.2 Crystals in $m\bar{3}$ Point Group

There are differences in the nonlinear properties of cubic crystals in the $m\bar{3}$ and $m\bar{3}m$ point groups. Figure 11 shows nonlinearity matrices plotted as a function of direction in the (111) for selected cubic crystals in the $m\bar{3}$ point group. Note that the phase of the nonlinearity matrix elements are periodic every 120° but are *not* symmetric about each bisector of the 120° period. Crystals in the $m\bar{3}$ point group differ from crystals in the $m\bar{3}m$ point group in that they have only twofold rotation symmetry about crystalline axes $\langle 100 \rangle$ instead of fourfold rotation symmetry and do not have twofold rotation symmetry about the face diagonals $\langle 110 \rangle$ [5]. In terms of elastic constants, both point groups have three independent second-order elastic constants, but in the $3\bar{m}$ point group $d_{112} = d_{133} = d_{223}$ differ from $d_{113} = d_{122} = d_{233}$ and $d_{155} = d_{266} = d_{344}$ differ from $d_{166} = d_{244} = d_{355}$. As a result, there are eight independent third-order elastic constants instead of six.

Figure 12 shows the linear and nonlinear parameters for Cs-alum [reproducing the graphs of the nonlinearity matrix elements of Fig. 11 in graphs (a) and (b)]. Note that the phases of the the lower half-plane roots $l_3^{(n)}$ are symmetric about each bisector of their 120° period, in contrast to the magnitude and phases of the nonlinearity matrix elements. Similar effects are seen for the other alums shown in Fig. 11.

To show that the asymmetry of the phases ψ_{lm} in Fig. 12 is purely a nonlinear effect, simulations were run for a "pseudo-Cs-alum," a fictional material with the same density and elastic constants as Cs-alum except that d_{113} is set equal to d_{112} and d_{166} set equal to d_{155}. This makes pseudo-Cs-alum elastically equivalent to a crystal in the $m\bar{3}m$ point group. Figure 13 shows a comparison of the nonlinearity matrix elements for the two materials. Observe that the $|S_{lm}|$ and ψ_{lm} curves for pseudo-Cs-alum shift such that they are symmetric about the the bisector of the 120° period. Also note that while the change in d_{113} and d_{166} is only about 10%, the maxima of $|S_{lm}|$ increase by 50% and shift by about 12°.

In the (110) plane, the nonlinearity matrix elements are also generally complex-valued for crystals in the $m\bar{3}$ point group. Figure 14 shows plots of the magnitude and phase of nonlinearity matrix elements for the same materials as Fig. 11. While the magnitudes $|S_{lm}|$ are periodic every 180°, the phases ψ_{lm} are only periodic every 360°. In addition, both the magnitudes and phases are symmetric about the bisectors of each 180° interval. The physical implication is that nonlinear propagation is expected to be identical in the

directions [001] (0°) and [00$\bar{1}$] (180°) but different for the directions [1$\bar{1}$0] (90°) and [$\bar{1}$10] (270°). This asymmetry does not occur for crystals in the $m\bar{3}m$ point group because for those materials the nonlinearity matrix elements can all be written in real-valued form [1].

Figure 15 shows the linear and nonlinear SAW parameters for Cs-alum [reproducing the graphs of the nonlinearity matrix elements of Fig. 14 in graphs (a) and (b)]. In contrast to the (111) plane, all the parameters of linear SAWs (c/c_{ref}, $|B_j/B_0|$, ϕ_j, $|l_3^{(n)}|$, and $\arg[l_3^{(n)}]$) shown in Fig. 15 are periodic every 180°, while the phases of the nonlinearity matrix elements ψ_{lm} are not. Thus in this case it also appears that the difference in periodicity is strictly a nonlinear effect.

To make the difference clearer, simulations were run for the pseudo-Cs-alum material described above for SAWs in the (110) plane. Figure 16 shows a comparison of the nonlinearity matrix elements for the two materials. Note that in pseudo-Cs-alum the phase becomes periodic every 180° and the matrix elements become real-valued ($\psi_{lm} = 0°$ or $\psi_{lm} = 180°$), just like other materials in the $m\bar{3}m$ point group. Note also that the change in d_{113} and d_{166} of only about 10% causes the maxima of $|S_{lm}|$ to more than double and the phases ψ_{lm} to shift significantly.

References

[1] R. E. Kumon, "Nonlinear surface acoustic waves in cubic crystals," Ph.D. dissertation, The University of Texas at Austin, 1999.

[2] A. Lomonosov, P. Hess, R. E. Kumon, and M. F. Hamilton, "Periodicity of linear and nonlinear surface acoustic wave parameters in the (111) plane of cubic crystals," J. Acoust. Soc. Am. **110**, (2001), [in press].

[3] G. W. Farnell, "Properties of elastic surface waves," in *Physical Acoustics*, edited by W. P. Mason and R. N. Thurston (Academic Press, New York, 1970), Vol. 6, pp. 109–166.

[4] M. F. Hamilton, Yu. A. Il'inskii, and E. A. Zabolotskaya, "Nonlinear surface acoustic waves in crystals," J. Acoust. Soc. Am. **105**, 639–651 (1999).

[5] W. Borchardt-Ott, *Crystallography*, 2nd ed. (Springer-Verlag, New York, 1995).

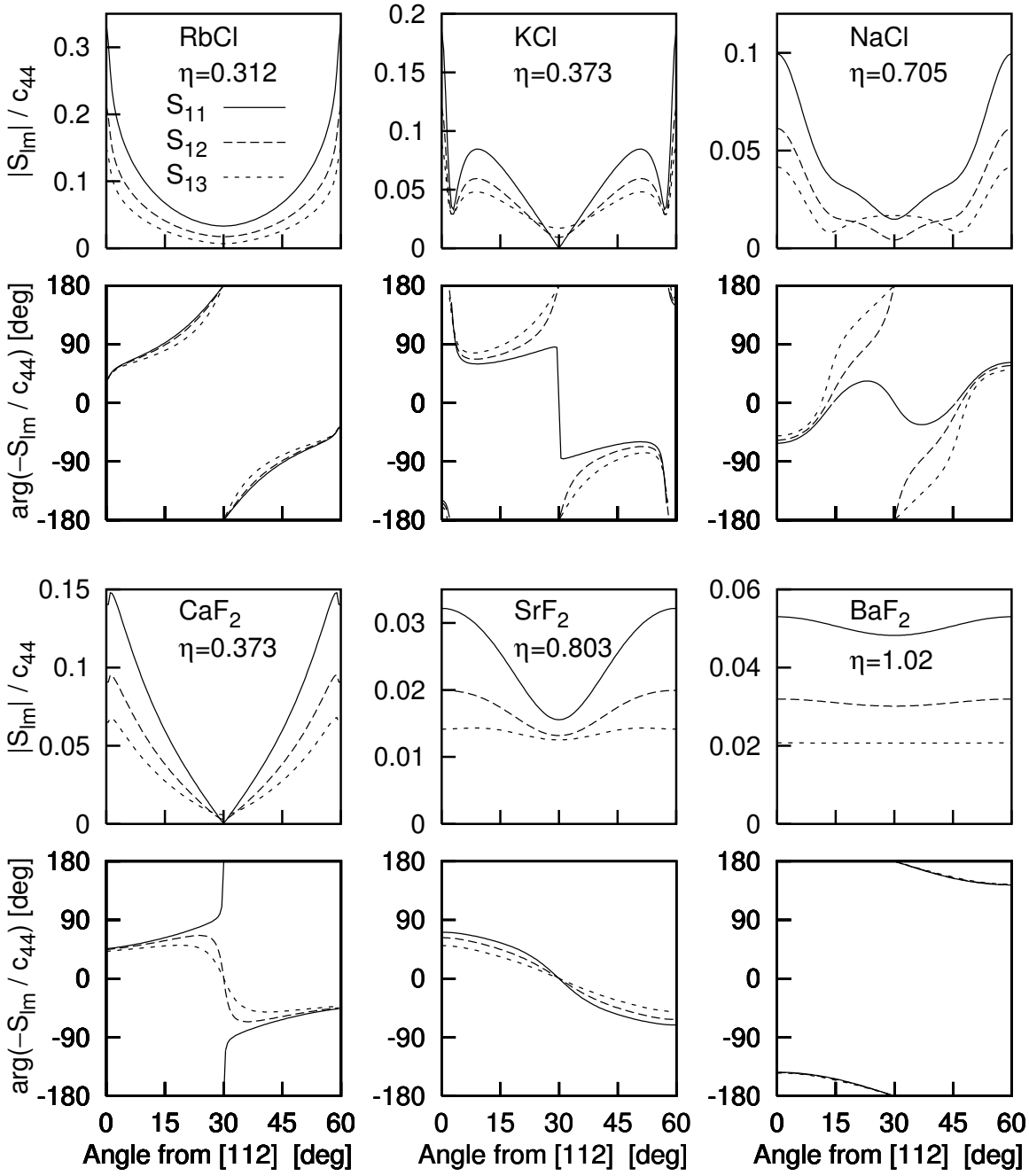

Figure 1: Dependence of nonlinearity matrix elements on direction of propagation in the (111) plane of selected materials in the $m\bar{3}m$ point group.

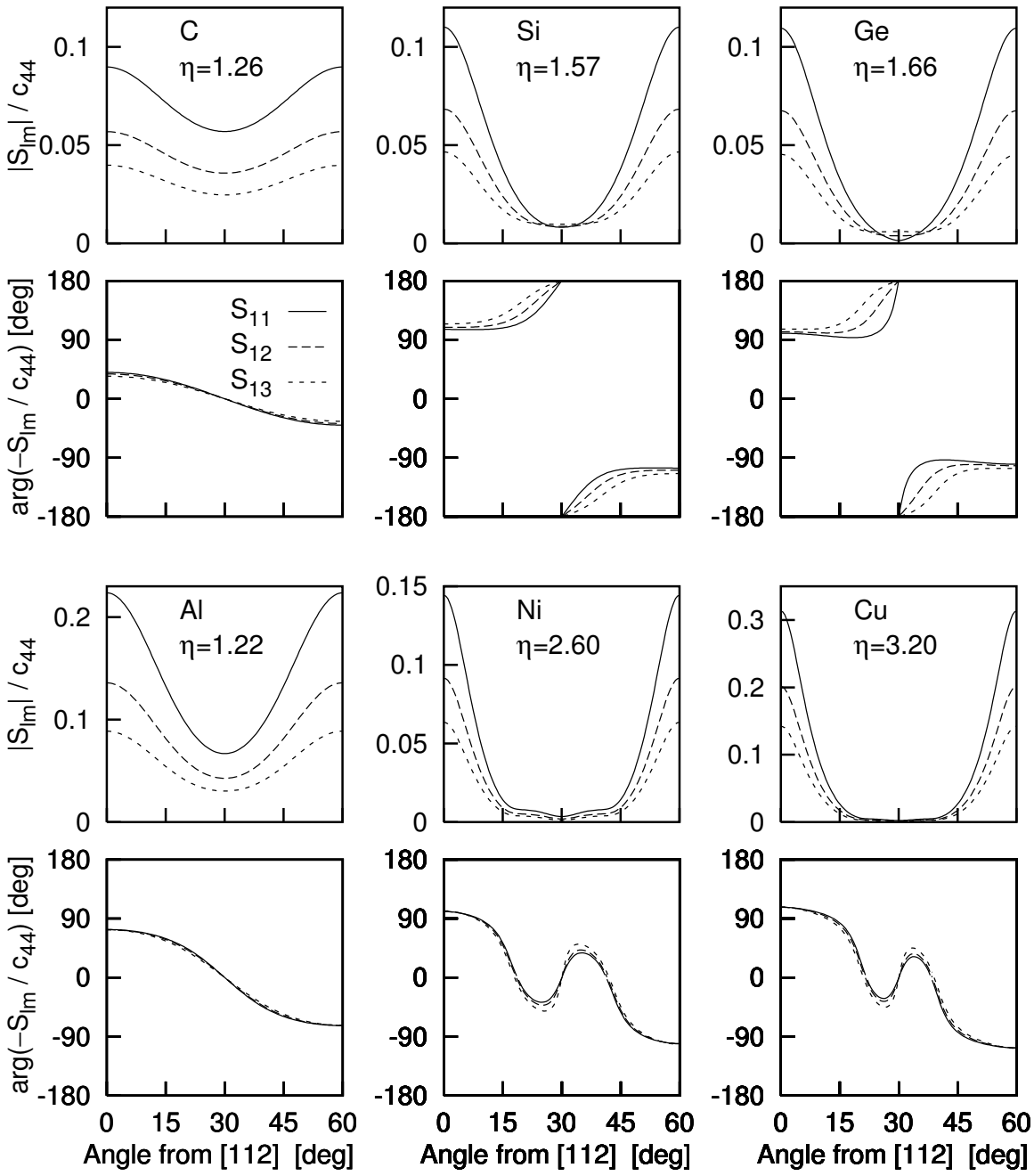

Figure 2: Dependence of nonlinearity matrix elements on direction of propagation in the (111) plane of selected materials in the $m\bar{3}m$ point group.

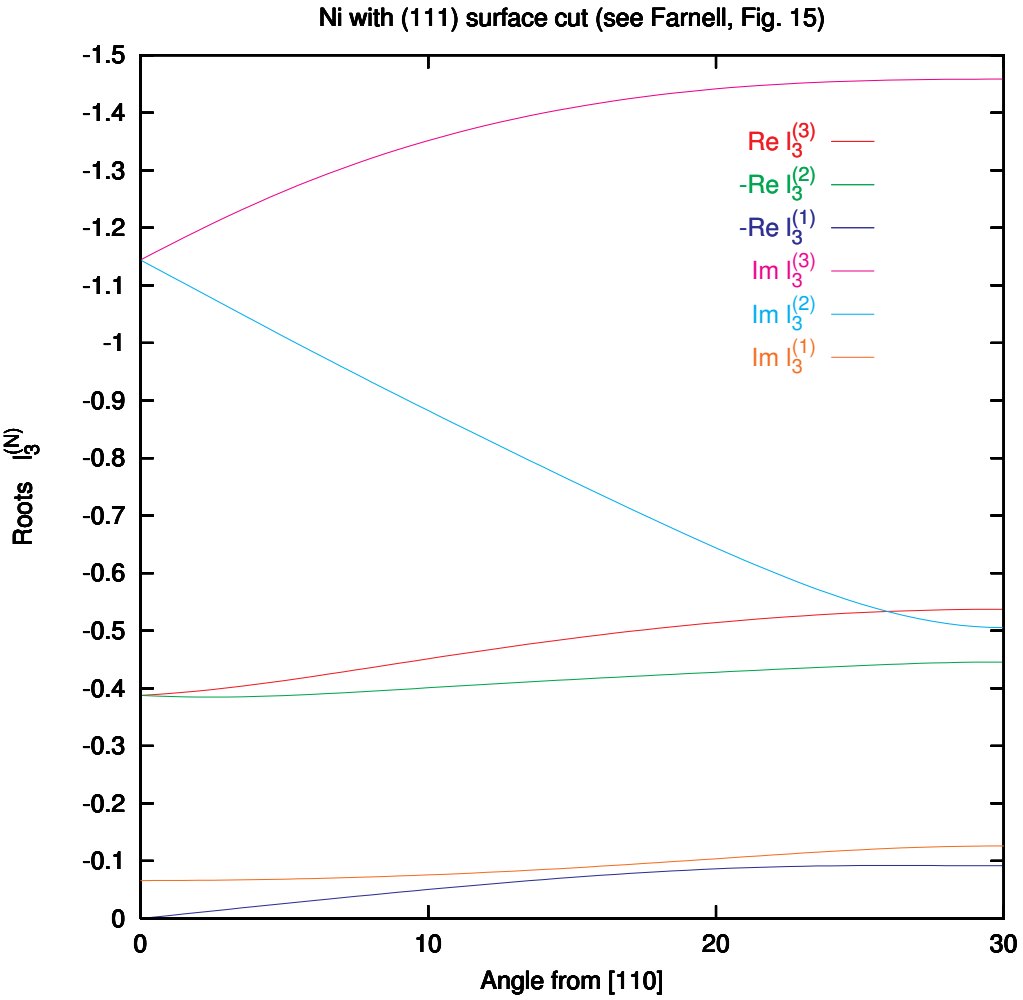

Figure 3: Lower half-plane roots for propagation on (111) plane of nickel over the range of directions 0° to 30° from [110]. (Compare with Fig. 15 in Farnell [3]). Note that the scale on the vertical axis is inverted.

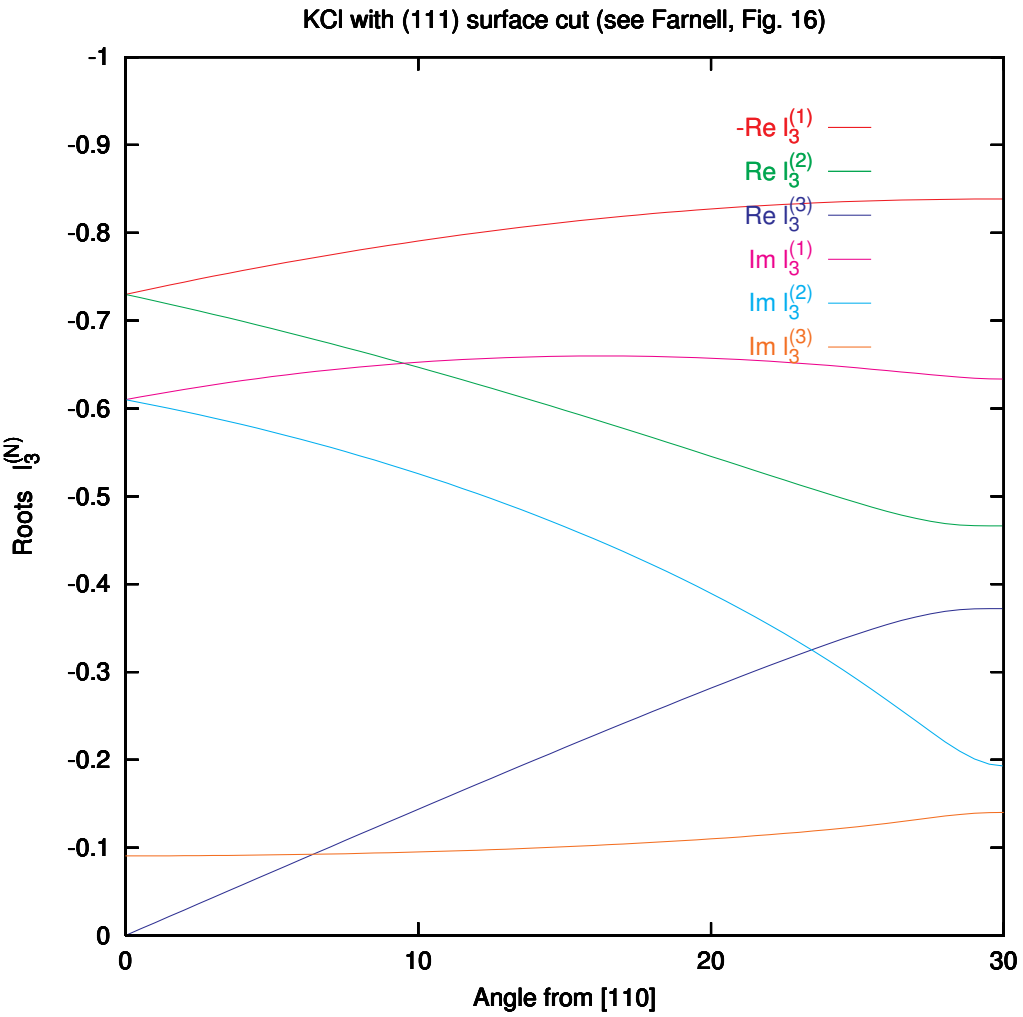

Figure 4: Lower half-plane roots for propagation on (111) plane of potassium chloride over the range of directions 0° to 30° from [110]. (Compare with Fig. 15 in Farnell [3]). Note that the scale on the vertical axis is inverted.

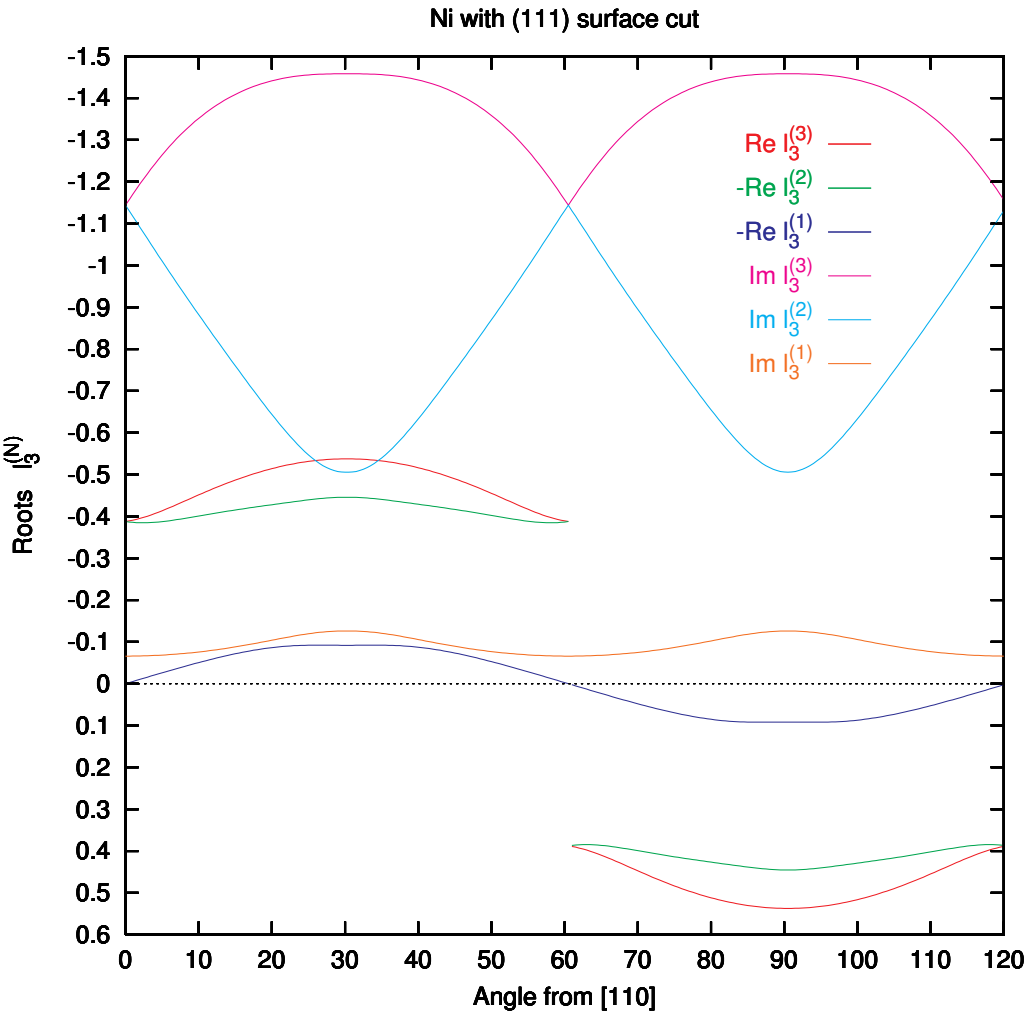

Figure 5: Lower half-plane roots for propagation on (111) plane of nickel over the range of directions 0° to 120° from [110]. The directions [112] and $[\bar{1}\bar{1}2]$ correspond to 30° and 90° on this graph. Note that the scale on the vertical axis is inverted.

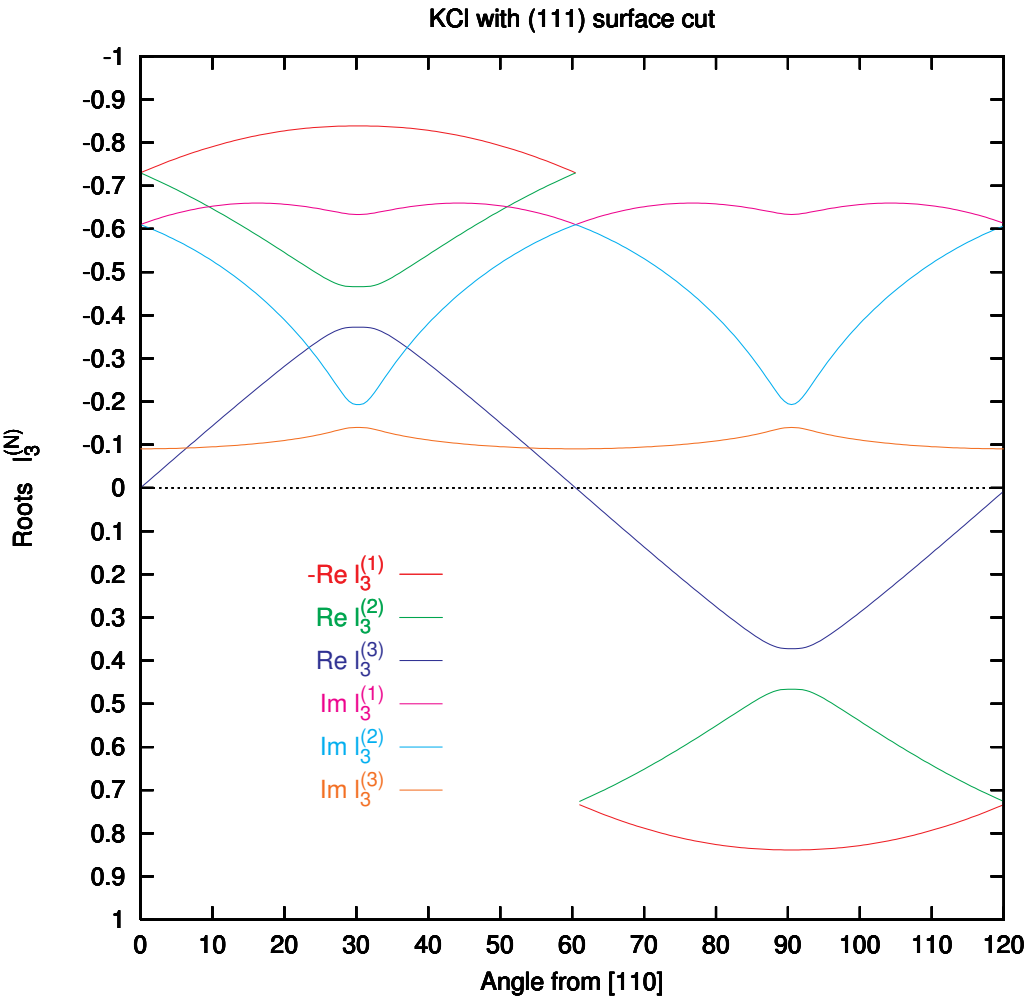

Figure 6: Lower half-plane roots for propagation on (111) plane of potassium chloride over the range of directions 0° to 120° from [110]. The directions [112] and $[\bar{1}\bar{1}\bar{2}]$ correspond to 30° and 90° on this graph. Note that the scale on the vertical axis is inverted.

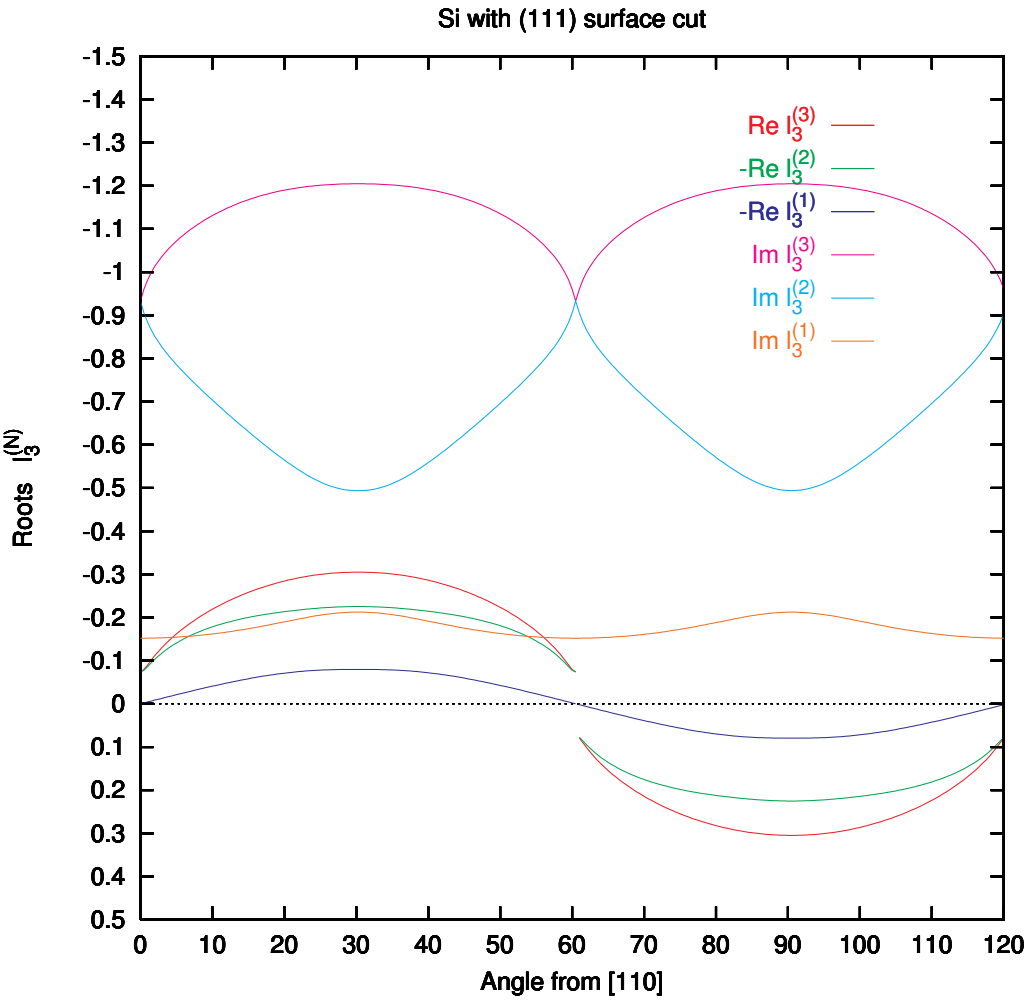

Figure 7: Lower half-plane roots for propagation on (111) plane of silicon over the range of directions 0° to 120° from [110]. The directions [112] and $[\bar{1}\bar{1}2]$ correspond to 30° and 90° on this graph. Note that the scale on the vertical axis is inverted.

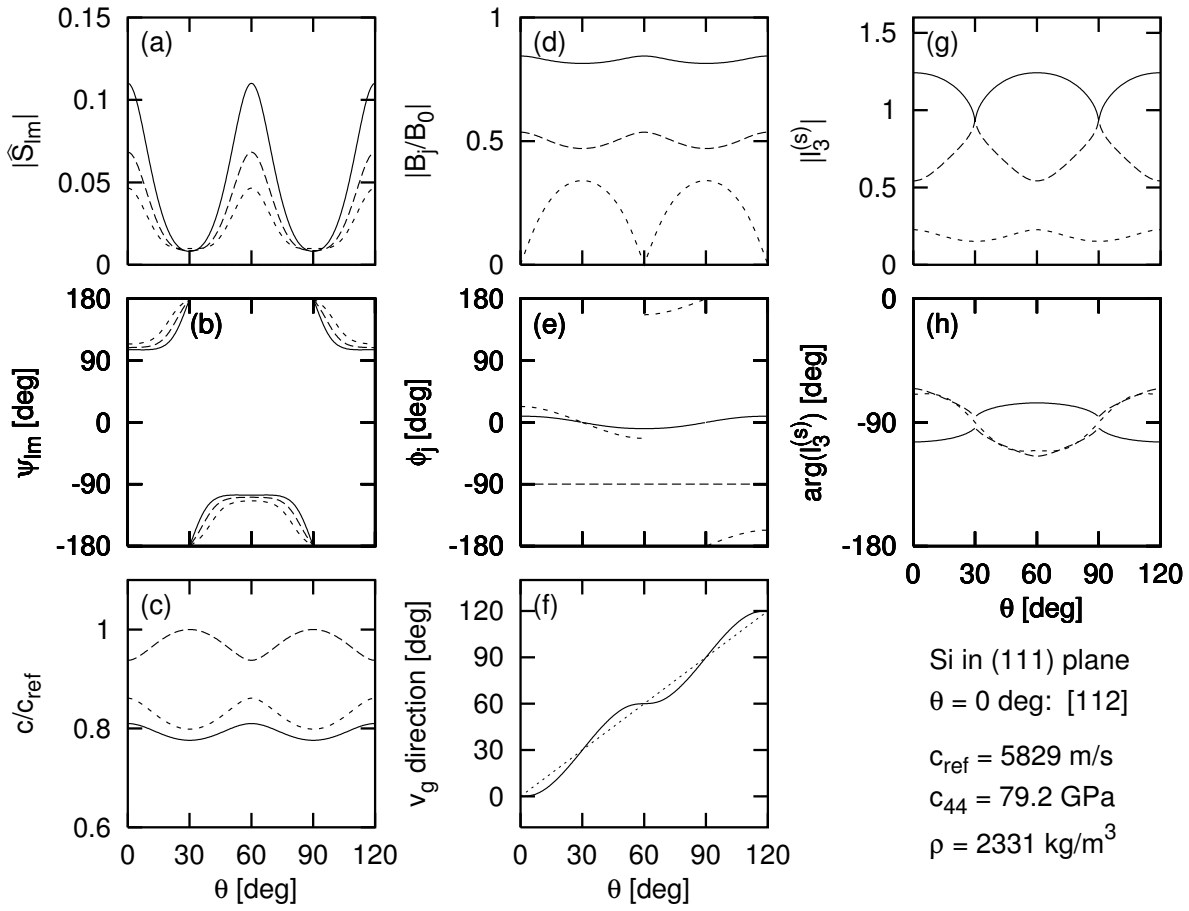

Figure 8: Dependence of linear and nonlinear parameters on the direction of propagation in the (111) plane of Si. The direction θ is measured in degrees from the $[11\bar{2}]$. The phases $\psi_{lm} = \arg(-S_{lm}/c_{44})$ and $\arg[l_3^{(s)}]$ are periodic every 120° and symmetric about the bisector of each 120° period. The phases $\phi_j = \arg(B_j/B_0)$ are periodic every 120°. All other parameters shown are periodic every 60° and symmetric about the bisector of each 60° period.

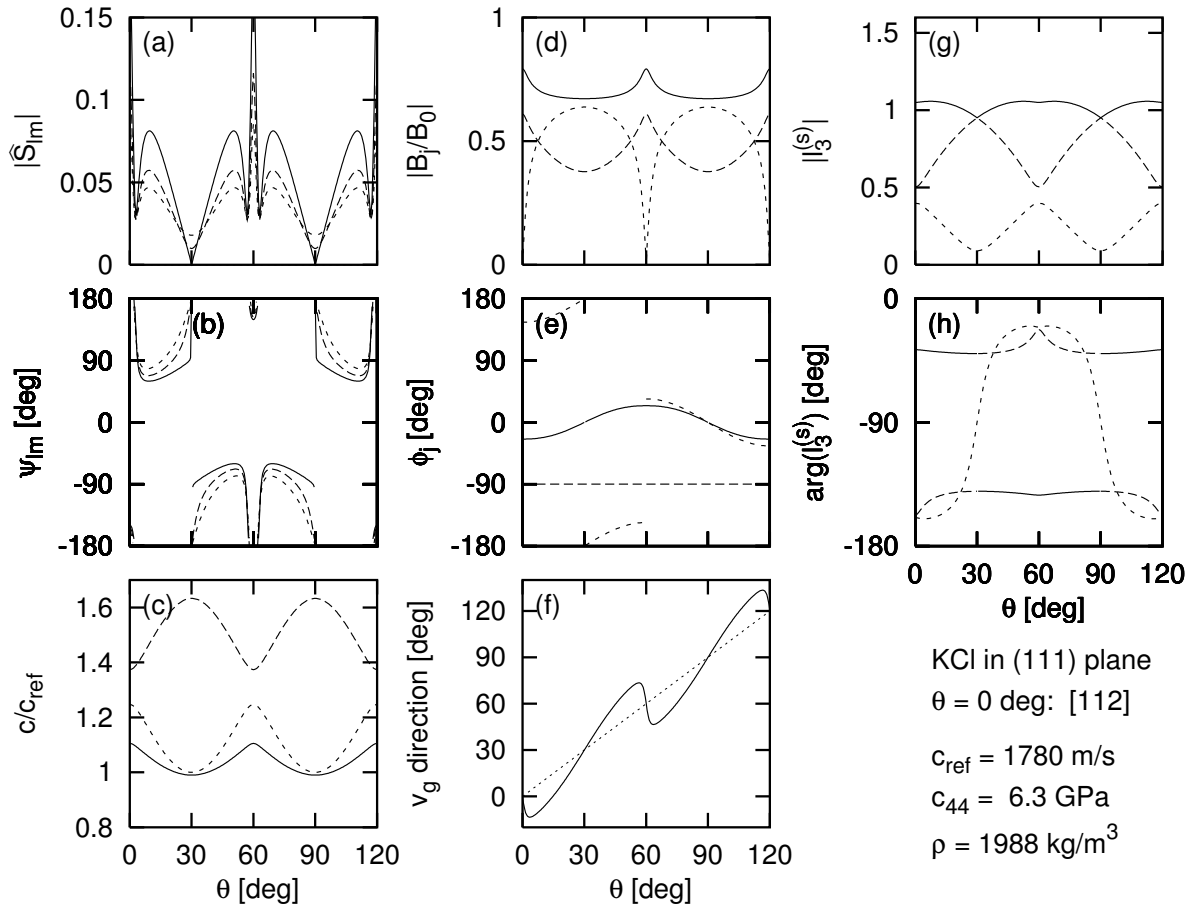

Figure 9: Dependence of linear and nonlinear parameters on the direction of propagation in the (111) plane of KCl. The direction θ is measured in degrees from the $[11\bar{2}]$. The phases $\psi_{lm} = \arg(-S_{lm}/c_{44})$ and $\arg[l_3^{(s)}]$ are periodic every 120° and symmetric about the bisector of each 120° period. The phases $\phi_j = \arg(B_j/B_0)$ are periodic every 120°. All other parameters shown are periodic every 60° and symmetric about the bisector of each 60° period.

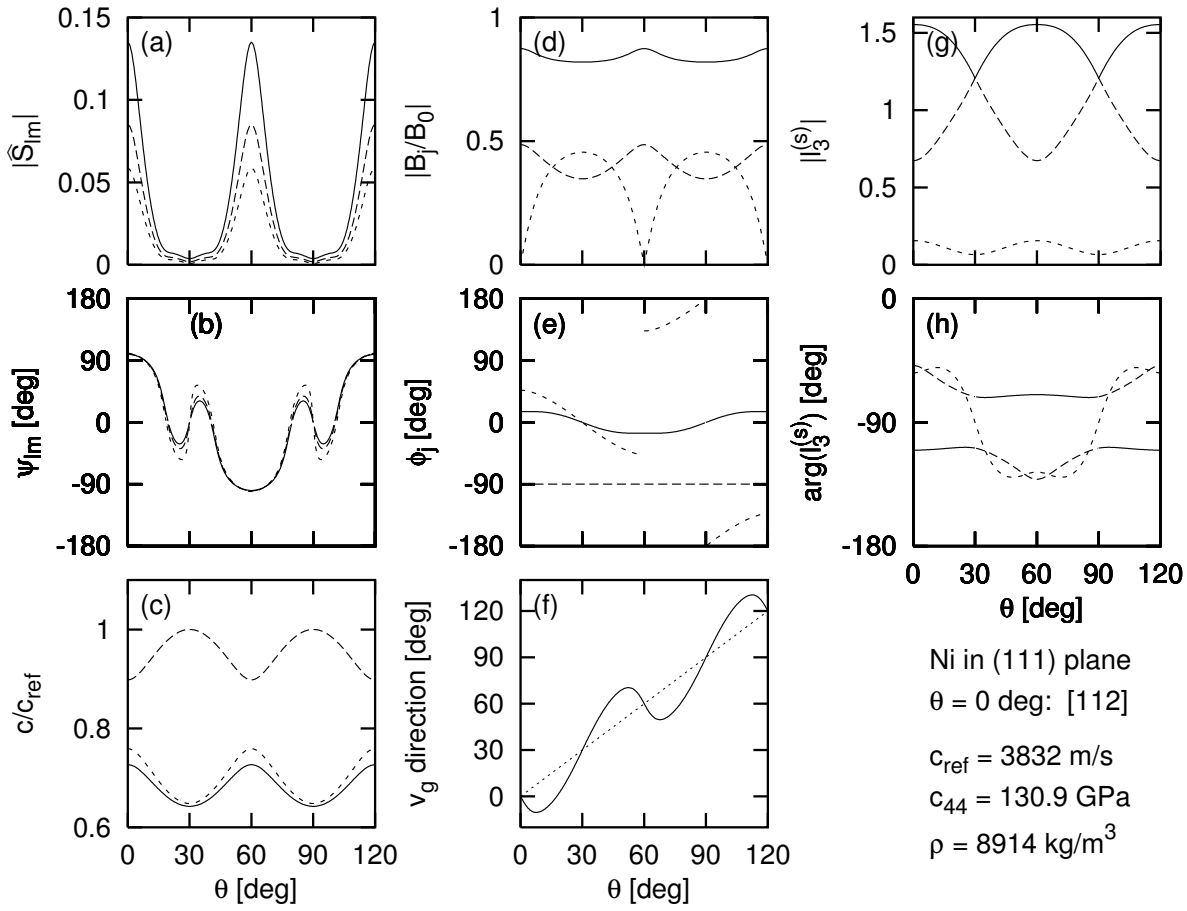

Figure 10: Dependence of linear and nonlinear parameters on the direction of propagation in the (111) plane of Ni. The direction θ is measured in degrees from the $[11\bar{2}]$. The phases $\psi_{lm} = \arg(-S_{lm}/c_{44})$ and $\arg[l_3^{(s)}]$ are periodic every 120° and symmetric about the bisector of each 120° period. The phases $\phi_j = \arg(B_j/B_0)$ are periodic every 120°. All other parameters shown are periodic every 60° and symmetric about the bisector of each 60° period.

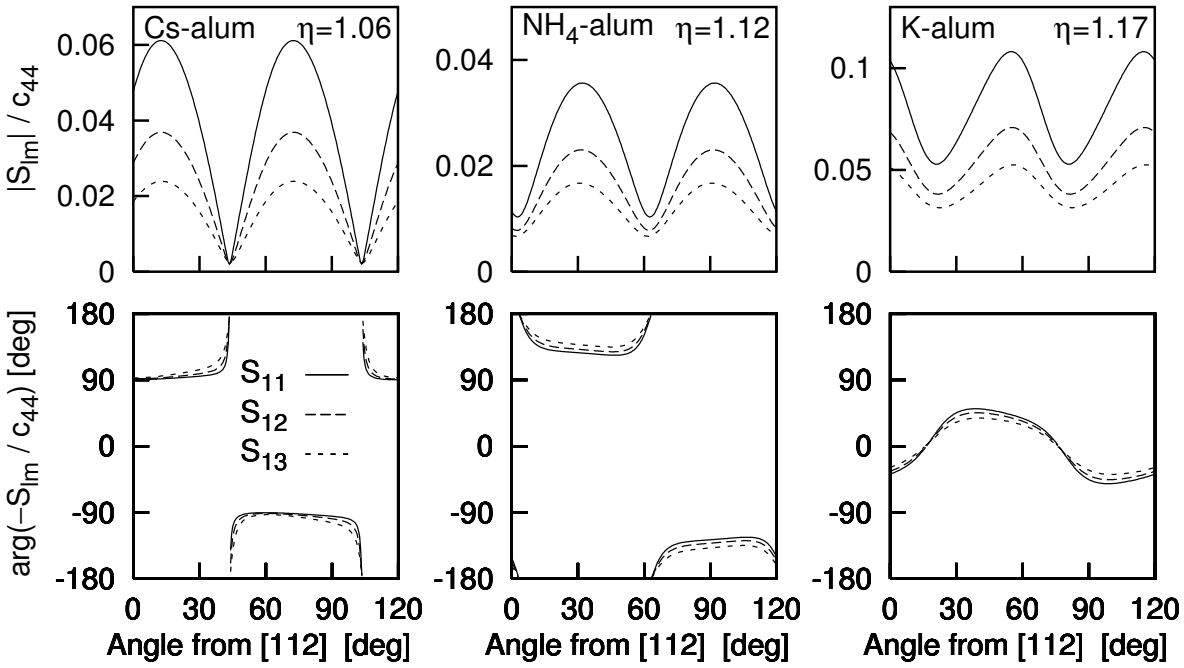

Figure 11: Dependence of nonlinearity matrix elements on direction of propagation in the (111) plane of selected materials in the $m\bar{3}$ point group. Note that the figures are plotted over the range from 0° to 120°, in contrast to Fig. 1 and 2.

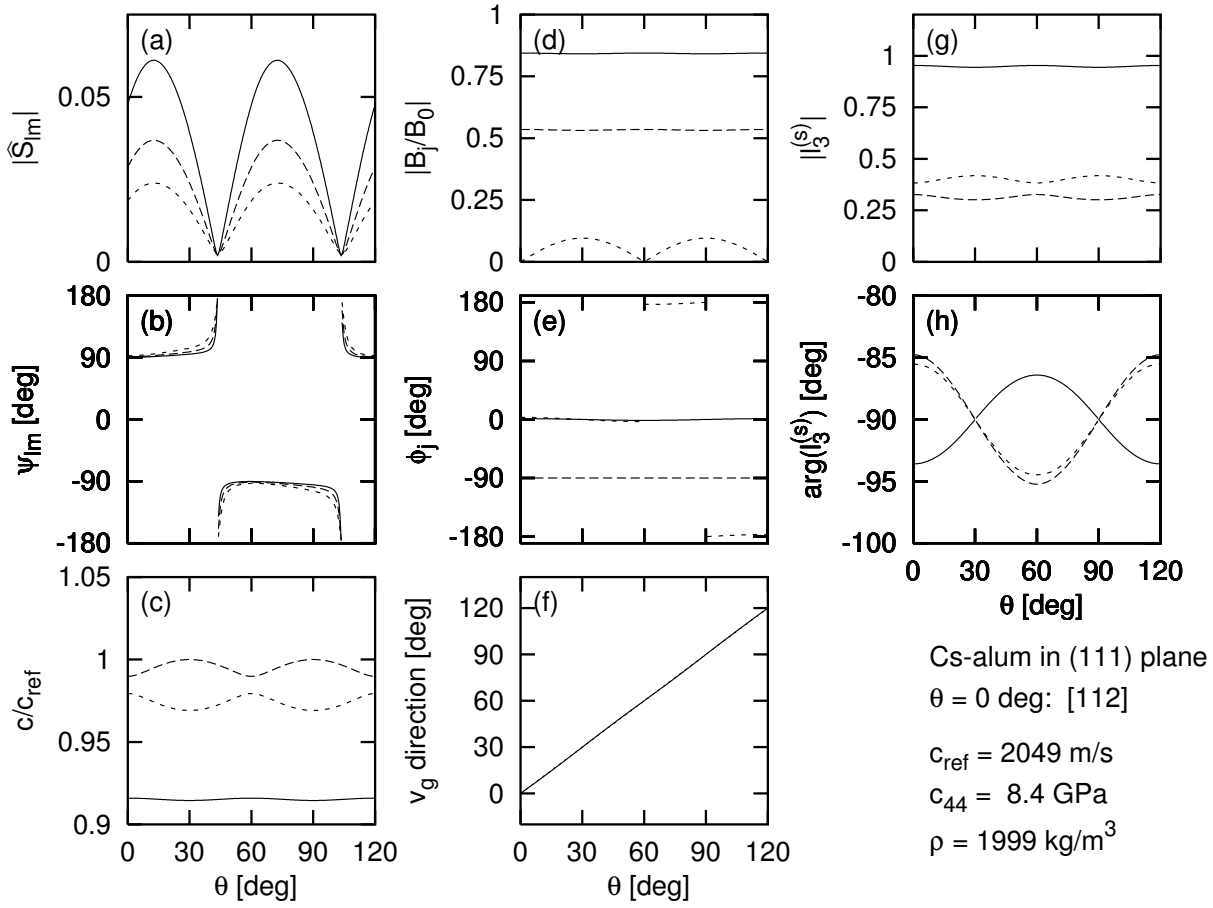

Figure 12: Dependence of linear and nonlinear parameters on the direction of propagation in the (111) plane of Cs-alum [$CsAl(SO_4)_2 \cdot 12\ H_2O$]. The direction θ is measured in degrees from the $[11\bar{2}]$. The phases $\psi_{lm} = \arg(-S_{lm}/c_{44})$ and $\arg[l_3^{(s)}]$ are periodic every 120°. However, only $\arg[l_3^{(s)}]$ is symmetric about the bisector of each 120° period. The phases $\phi_j = \arg(B_j/B_0)$ are periodic every 120°. All other parameters shown are periodic every 60° and symmetric about the bisector of each 60° period.

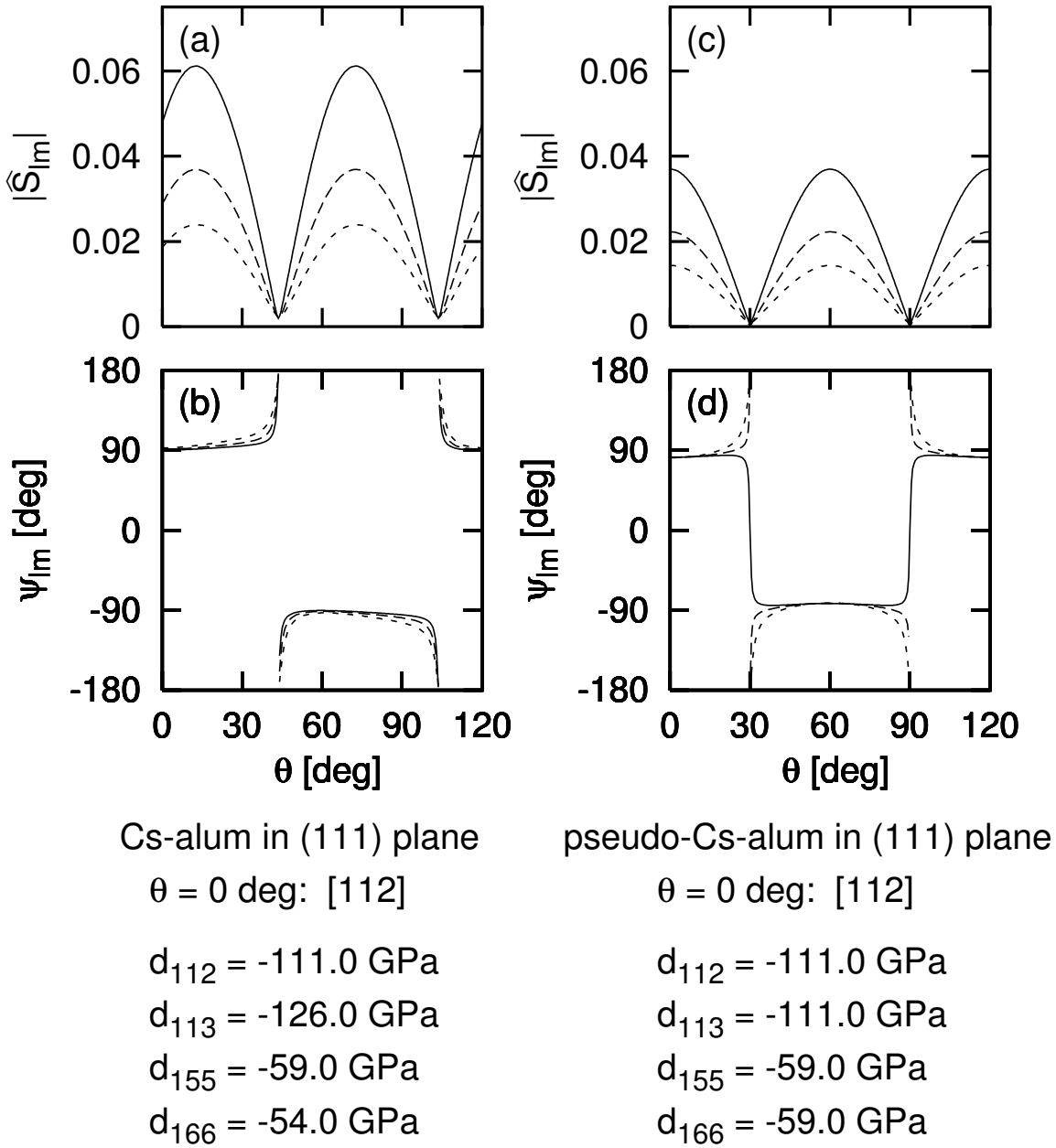

Figure 13: Dependence of nonlinearity matrix elements on direction of propagation in the (111) plane of Cs-alum and the fictional material "pseudo-Cs-alum." The two materials have all the same properties except for the differences in third-order elastic constants shown in the figure. Note the shift in the directions of the maxima of the magnitudes and the asymmetry of the phase with respect to the bisector of the 120° range.

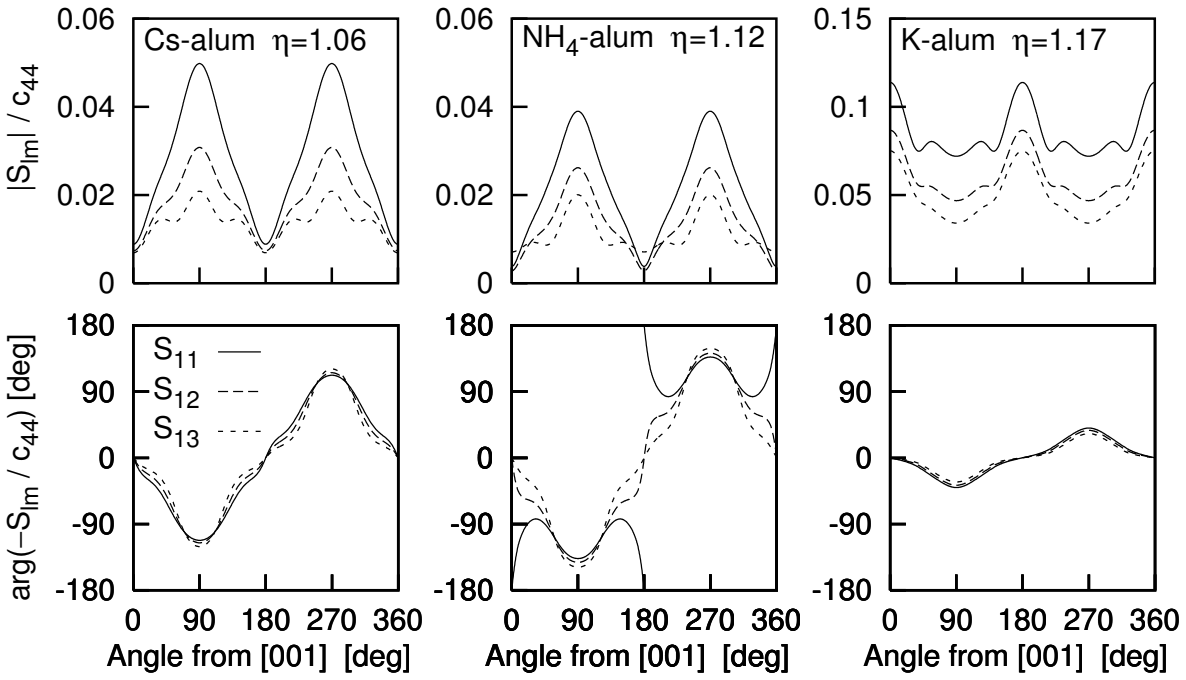

Figure 14: Dependence of nonlinearity matrix elements on direction of propagation in the (110) plane of selected materials.

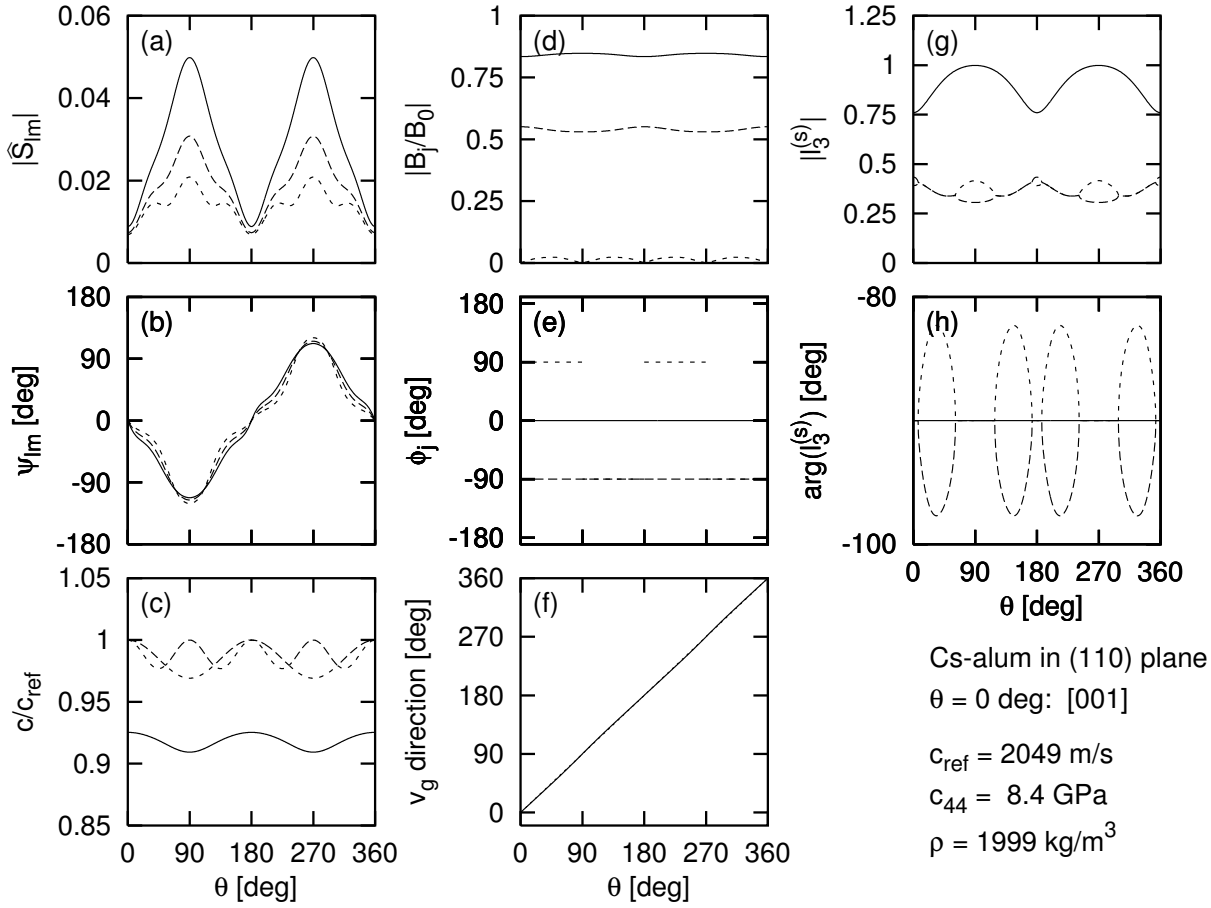

Figure 15: Dependence of linear and nonlinear parameters on the direction of propagation in the (110) plane of Cs-alum [$CsAl(SO_4)_2 \cdot 12\ H_2O$]. The direction θ is measured in degrees from the [001]. The phases $\psi_{lm} = \arg(-S_{lm}/c_{44})$ are periodic every 360°. However, all the other parameters shown are periodic every 180°. In addition, all the parameters except ϕ_j are symmetric about the direction $\theta = 90°$ over $0 \leq \theta \leq 180°$ and about the direction $\theta = 270°$ over $180 \leq \theta \leq 360°$.

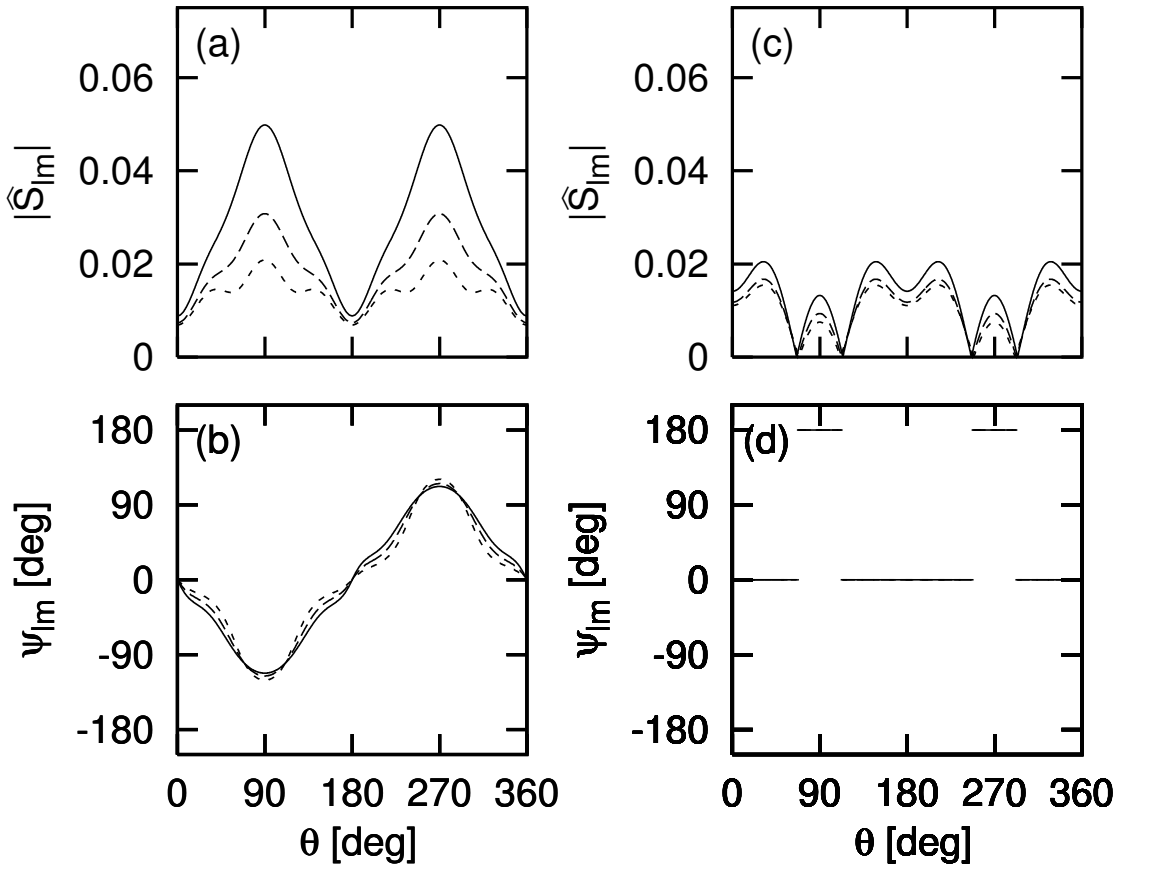

Figure 16: Dependence of nonlinearity matrix elements on direction of propagation in the (110) plane of Cs-alum and the fictional material "pseudo-Cs-alum." The two materials have all the same properties except for the differences in third-order elastic constants shown in the figure. Note that the phase becomes periodic every 180° as the matrix elements become real-valued.

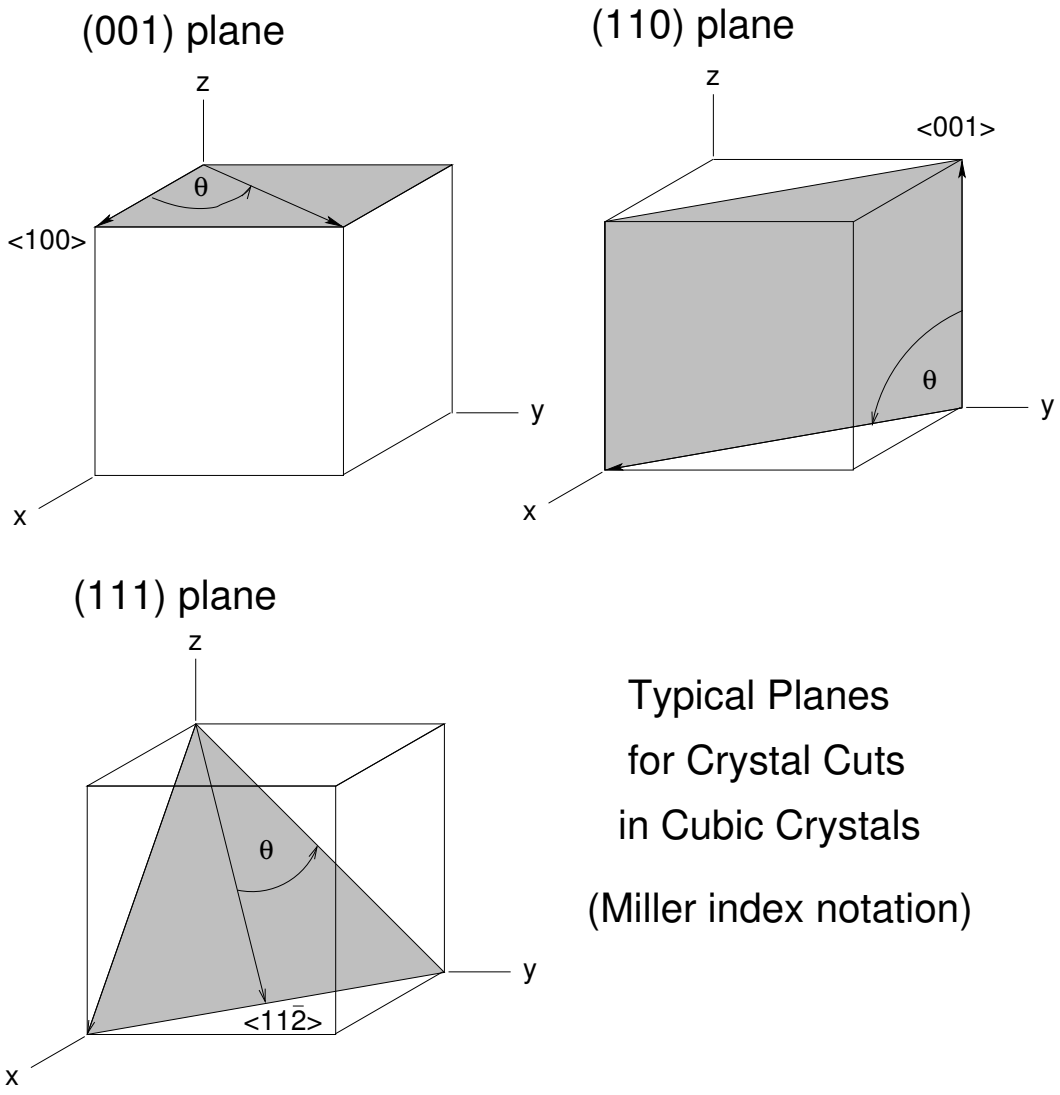

Figure 17: Typical planes for crystal cuts in cubic crystals as specified using Miller index notation. The reference directions used for specifying directions of propagation are indicated by the vector direction in angle brackets.